

Adaptive Point Transformer

Alessandro Baiocchi^{a,*}, Indro Spinelli^b, Alessandro Nicolosi^c, Simone Scardapane^d

^a*Sapienza University of Rome, Department of Computer, Control and Management Engineering, Via Ariosto 25, Rome, 00185, Italy*

^b*Sapienza University of Rome, Department of Computer Science, via Salaria, 113, Rome, 00198, Italy*

^c*Leonardo Labs, Piazza Monte Grappa, 4, Rome, 00195, Italy*

^d*Sapienza University of Rome, Department of Electronics and Telecommunication Engineering, via Eudossiana, 18, Rome, 00184, Italy*

Abstract

The recent surge in 3D data acquisition has spurred the development of geometric deep learning models for point cloud processing, boosted by the remarkable success of transformers in natural language processing. While point cloud transformers (PTs) have achieved impressive results recently, their quadratic scaling with respect to the point cloud size poses a significant scalability challenge for real-world applications. To address this issue, we propose the Adaptive Point Cloud Transformer (AdaPT), a standard PT model augmented by an adaptive token selection mechanism. AdaPT dynamically reduces the number of tokens during inference, enabling efficient processing of large point clouds. Furthermore, we introduce a budget mechanism to flexibly adjust the computational cost of the model at inference time without the need for retraining or fine-tuning separate models. Our extensive experimental evaluation on point cloud classification tasks demonstrates

*Email: alessandro.baiocchi@uniroma1.it

that AdaPT significantly reduces computational complexity while maintaining competitive accuracy compared to standard PTs. The code for AdaPT is made publicly available.

Keywords: Transformer, Geometric Deep Learning, Point Clouds, Gumbel-Softmax, Token Selection

1. Introduction

The increasing ubiquity of point cloud data across diverse domains, from autonomous navigation to environmental monitoring, has spurred significant advancements in point cloud representation learning (Camuffo et al., 2022). Unlike traditional two-dimensional data, point clouds exhibit unique characteristics, including their inherent invariance under the permutation of their constituent points. These properties pose inherent challenges for conventional neural network architectures, necessitating the development of tailored methodologies specifically designed for point cloud processing.

Early attempts to tackle point cloud analysis relied on localized message-passing approaches inspired by graph neural networks (Kipf and Welling, 2017), as exemplified by PointNet (Charles et al., 2017) and its extensions (Qi et al., 2017; Guo et al., 2020). However, these methods often suffer from limited receptive field sizes, particularly when dealing with large-scale point clouds.

In recent years, the adoption of transformers (Vaswani et al., 2017), initially introduced for natural language processing, has emerged as a promising alternative for point cloud representation learning (Guo et al., 2021). Transformers excel in handling unordered data through their attention mechanism,

which operates on tokenized representations of the input data. This tokenization enables transformers to readily adapt to diverse data types, treating each token as an independent entity, regardless of its origin. After the tokenization, the self-attention mechanism is crucial in preserving the permutation invariance of point clouds. By operating on an unordered set of tokens, self-attention allows transformers to learn relationships between points without explicitly considering their order. However, the quadratic computational complexity of self-attention poses a significant challenge for scaling transformers to large point clouds (Hackel et al., 2017). Several approaches have been proposed to mitigate this issue. One strategy involves using a fixed number of tokens by grouping multiple points into single tokens (Guo et al., 2021). This method offers computational efficiency but sacrifices accuracy due to the aggregation of heterogeneous points. Another approach involves knowledge distillation, where a large, pre-trained model (teacher) is used to train a smaller, more efficient model (student) (Zhang et al., 2023; Yao et al., 2022). This approach can reduce inference time at the cost of reduced accuracy.

Token selection, another technique for reducing token count, involves selectively eliminating tokens based on a relevance criteria. This method has been successfully employed in computer vision applications, such as AdaViT (Meng et al., 2022) and DynamicViT (Rao et al., 2021), which dynamically assess token importance for the main tasks. Yang et al. (Yang et al., 2019) adapted this framework for point cloud preprocessing. However, these methods require users to pre-define a token budget, limiting flexibility.

To address these shortcomings, we propose the Adaptive Point Cloud

Transformer (AdaPT), a novel model that seamlessly integrates adaptive downsampling and dynamic resource allocation. AdaPT adaptively selects the number of tokens to retain based on an input parameter specified at inference time, enabling a flexible trade-off between computational resources and prediction accuracy. AdaPT’s ability to adjust its computational budget based on available resources makes it well-suited for real-world applications where resource constraints necessitate efficient processing with variable inference time, especially when dealing with variable-sized point clouds. The proposed AdaPT model represents a significant step in developing scalable and adaptable point cloud representation learning methods.

Organization of the paper

After introducing AdaPT in Section 3, we demonstrate its effectiveness through extensive experiments in Section 4. In Section 4.4 we provide an in-depth analysis of AdaPT’s performance and several ablation studies to validate its performance in handling large-scale point clouds with varying computational budgets. We conclude in 5 with some final remarks and possible future directions.

2. Related Works

In this section, we present related works on two aspects: Point Cloud processing and Transformer-based models.

2.1. Point Cloud Representation and Processing

PointNet is considered the pioneering work in point cloud learning (Charles et al., 2017), followed by PointNet++ (Qi et al., 2017). These models di-

rectly process point cloud data and learn a representation of the input using a feed-forward network, which is applied independently to each point. The information from all points is then aggregated in a permutation-invariant manner. PointNet++ enhances this approach by introducing local features obtained by aggregating information from neighboring points through ball query grouping and a hierarchical PointNet structure.

Several other works have defined a convolution operator for point clouds. These models typically leverage voxelization or octrees. The former approach converts point cloud data into a regular three-dimensional voxel structure, facilitating standard convolution. The latter approach uses a tree structure combined with varying sizes of voxels to capture different densities within the point cloud. Notable examples of these models include SparseConvNet (Graham et al., 2018) and OctNet (Riegler et al., 2017), which exploit the natural sparsity of input point clouds. However, these techniques are limited by the local receptive field of the convolution operator, which may be insufficient for large-scale point clouds.

To address this limitation, Wang et al. (2019) introduced the EdgeConv operator, which enables dynamic convolution over the point cloud and captures both global and local information. Despite these advancements, convolutional approaches still underperform compared to attention-based counterparts (Guo et al., 2021), a topic we discuss in the following subsection.

2.2. Transformer Architectures

Transformer models, introduced by Vaswani et al. (2017), were initially designed for natural language processing (NLP) tasks, exploiting the attention mechanism. These models operate on tokens derived from the input

through a tokenization operation. The tokens are processed to obtain a hidden representation, typically by a task-specific head, to yield the final prediction.

The high parallelization possible in attention calculations has allowed transformer models to benefit significantly from recent GPU performance improvements, enabling larger models' training (Narayanan et al., 2021).

Following their introduction in NLP, the general nature of their architecture has allowed transformers to be employed across various fields, achieving outstanding performance (Islam et al., 2024). Typically, the only adjustment needed for a transformer to work with different data types is to replace the initial tokenization module.

In image processing, for example, Vision Transformers (ViTs) have replaced Convolutional Neural Networks as the state-of-the-art for various tasks, such as image classification and image segmentation (Dosovitskiy et al., 2021; Thisanke et al., 2023).

Graph Transformers (GTs) (Müller et al., 2023), a family of architectures based on transformers, have been developed to operate on graph-structured data, leveraging the desirable properties of the attention operation.

Transformer-based models have recently emerged in point cloud data processing (Zeng et al., 2022). In particular, Guo et al. (2021) and Zhao et al. (2021) simultaneously introduced a transformer-based model for point cloud data. Transformers inherently possess desirable properties for point cloud deep learning, as they naturally maintain permutation invariance among the tokens, treating them as an unordered set.

Due to the inherently quadratic nature of the attention operation (Du-

man Keles et al., 2023), scaling the number of tokens used in transformers is challenging. One solution involves developing dynamic models capable of subsampling only the most relevant tokens in the input.

In the field of image processing, models such as AdaViT (Meng et al., 2022) and DynamicViT (Rao et al., 2021) have been developed, proposing methods for selecting and removing unimportant tokens during the calculations.

In the context of point cloud data, recent works, such as that by Yang et al. (2019), employ strategies analogous to those used in ViTs to subsample less relevant tokens.

Existing models have successfully enhanced the performance and interpretability of their base models, albeit at the cost of some accuracy. These models, applicable to images and point clouds, necessitate the pre-determination of a computational budget, establishing a fixed trade-off at inference time. The contribution we introduce in the subsequent section offers a significant advancement over these models. Our approach allows for an adaptive computational budget at inference time, enabling a dynamic trade-off between accuracy and computational complexity. Importantly, this adaptability is achieved without the need to re-train the model.

3. Adaptive Point Transformer

In this work, we present the Adaptive Point Transformer (AdaPT), a model capable of classifying point cloud data using a flexible computational budget at inference time. To achieve this, we pair a series of transformer layers with a set of token selection modules. These modules subsample,

in a differentiable manner, the tokens used in the point cloud transformer, reducing the computational effort needed in subsequent layers.

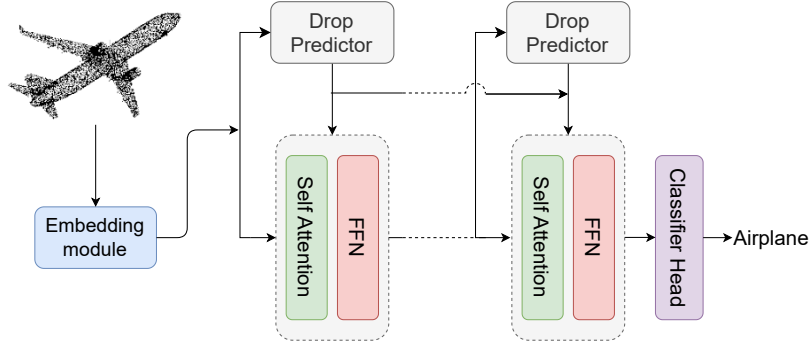


Figure 1: Architecture of the AdaPT model. The embedding module consists of an Absolute-Relative positional embedding (Yang et al., 2019). The transformer blocks are paired with the proposed *drop predictors*. Finally, the representation is processed by a classifier head which outputs a prediction.

The amount of tokens sampled at each layer is not fixed. This allows for the computational budget available to the model to be decided at inference time for each data point. In the following sections, we explain the components of the model, which are shown schematically in Fig. 1.

3.1. Point Cloud Transformer

We want to build a transformer-based architecture in order to be able to drop less relevant tokens in a similar manner to Rao et al. (2021). We need our point cloud data to be embedded in tokens to employ a transformer model. We do this through the Absolute-Relative Positional Embedding (ARPE) module presented in Yang et al. (2019). This module embeds each point into a token utilizing information from the point itself and its nearest neighbors. Let $x \in \mathbb{R}^{N \times F}$ be a point cloud made of N points, each with f

features. Let $k_i \in \mathbb{R}^{k \times F}$ be the set of k nearest points to a point $x_i \in x$. The embedding is done as follows:

$$\text{ARPE}(x_i) = \gamma(\max\{h(x') \mid x' \in k_i\})$$

where both γ and h are Multi-Layer Perceptrons (MLPs) with group normalization and ELU activation (Clevert et al., 2016).

The tokens are then processed by a series of transformer layers employing multi-head attention (MHA), layer normalization (LN), and a MLP composed of two linear layers with GELU activations:

$$\begin{aligned} z_0 &= \text{ARPE}(x_i) \\ z_\ell &= \text{MLP}(\text{LN}(\text{MHA}(\text{LN}(z_{\ell-1})))) \end{aligned}$$

The final token representations are averaged, and the result is passed through a classification head made of a MLP composed of two linear layers with GELU activations, which outputs the network’s prediction:

$$z'_f = \frac{1}{n} \sum_{i=0}^n z_{f,i} \quad y = \text{MLP}(z'_f)$$

where z'_f is the average computed over the final tokens.

3.2. Drop predictor module

The main aim of the AdaPT model is to reduce the computational effort during inference by subsampling the tokens. This is done through modules responsible for the token selection, which are called “drop predictors”, whose architecture is shown in Fig. 2. These modules take into consideration both local (relative to the single token) and global (relative to all tokens) features.

Let $x \in \mathbb{R}^{n \times F}$ be the input tokens to a drop predictor layer. We first compute what we call local and global features as:

$$z_{local} = \text{MLP}(x) \in \mathbb{R}^{n \times F'} \quad z_{global} = \text{Agg}(\text{MLP}(x)) \in \mathbb{R}^{F'}$$

where Agg is an aggregation operation, e.g. average pooling, and F' is an arbitrary dimension, in our case, $F' = F/2$. The global features are repeated n times, obtaining a new $z_{global} \in \mathbb{R}^{n \times f'}$. These features are concatenated and fed to an additional MLP that predicts the probabilities of keeping the tokens:

$$z = [z_{local}, z_{global}] \in \mathbb{R}^{n \times F} \quad \pi = \text{Softmax}(\text{MLP}(z)) \in \mathbb{R}^{n \times 2}$$

where $\pi_{i,0}$ denotes the probability of eliminating the i -th token, while $\pi_{i,1}$ denotes the probability of keeping it.

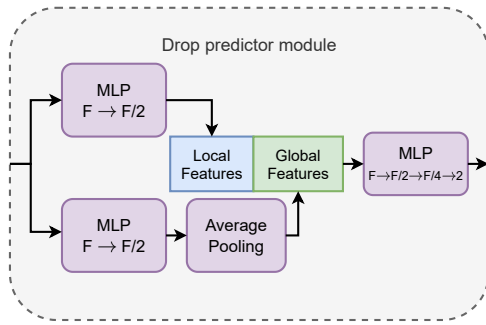


Figure 2: Scheme of the drop predictor module architecture.

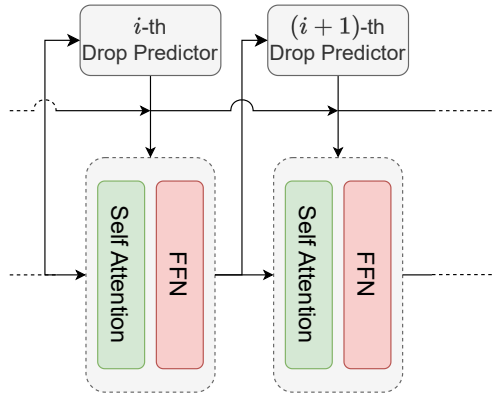


Figure 3: Drop predictor modules usage in the PCT.

We also want the model to learn to select the least relevant tokens for a given task and eliminate them. For end-to-end training to be possible, we

need to sample the tokens in a differentiable manner. This is done by employing the Gumbel-Softmax (GS) estimator (Jang et al., 2017) to differentially sample from the probability distributions $\pi_j \in \mathbb{R}^2; j = 1, \dots, N$:

$$\text{GS}(\pi_j, \tau)_i = \frac{\exp((\log(\pi_{j,i}) + g_{j,i})/\tau)}{\sum_{k=0,1} \exp((\log(\pi_{j,k}) + g_{j,k})/\tau)} \quad i = 0, 1; j = 0, \dots, N \quad (1)$$

where $g_{i,j}$ are i.i.d. samples drawn from $\text{Gumbel}(0,1)$ ¹, and τ is the temperature parameter, which is set to $\tau = 1$ in our experiments.

To obtain a binary output an argmax is applied during the forward pass, while straight-through estimation (Jang et al., 2017) is used for the computation of the gradients. We obtain the binary mask $D \in \{0, 1\}^N$ we use to index the tokens as:

$$D_j = \text{argmax}(\text{GS}(\pi_j, \tau))_1 \in \{0, 1\} \quad j = 1, \dots, N \quad (2)$$

We use only the values corresponding to keeping the tokens so that D can be used directly as a boolean mask to index the tokens. We add drop predictor modules to a subset of the transformer blocks in the PCT, as shown in Fig. 3.

During the training phase, the tokens are not eliminated; they are instead masked in the attention, effectively preventing them from contributing to the prediction in successive steps. At inference time, the tokens are completely removed, boosting the computational efficiency in the successive layers. A demonstration of the effect of this token elimination is shown in Fig. 4. Each

¹The Gumbel distribution samples can be drawn by computing $g = -\log(-\log(u))$, where u is drawn from $\text{Uniform}(0,1)$.

drop predictor module also passes its decision on which tokens to eliminate to the next layers in such a way as to ensure that, during the training phase, once a token is masked, it stays masked for all of the remaining computations.



Figure 4: Visualization of the kept tokens along the model’s layers for a few representative examples.

Additionally, we add a regularization term to the loss to incentivize the model to drop tokens. We describe the regularization term for a single budget here, and its extension to a flexible budget in the next section. Denote by t_i the target ratio of dropped tokens for the i -th drop predictor. The regularization term we consider is the following:

$$\mathcal{L}_{drop} = \sum_{i=0}^p \frac{(d_i - t_i)^2}{p} \quad (3)$$

where p is the total number of drop predictors, while d_i and t_i are the fraction of token dropped and the target drop ratio for the i -th drop predictor.

This regularization term is added to a standard cross entropy loss term

\mathcal{L}_{CE} . The complete loss function is then:

$$\mathcal{L} = \mathcal{L}_{CE} + \alpha \mathcal{L}_{drop} \quad (4)$$

where α is a parameter controlling the strength of the regularization.

3.3. Flexible budget

Finally, we want our trained model to be able to operate with multiple computational budgets, which are to be selected by the user at inference time. To achieve this, we add to the model multiple sets of drop predictors in parallel, one for each desired budget. Note that each drop predictor layer (as described in Section 3.2) is extremely small, thus adding a low overhead of parameters to the complete model. These B sets of drop predictors are all trained simultaneously while sharing the same backbone model. This is shown schematically in Fig. 5.

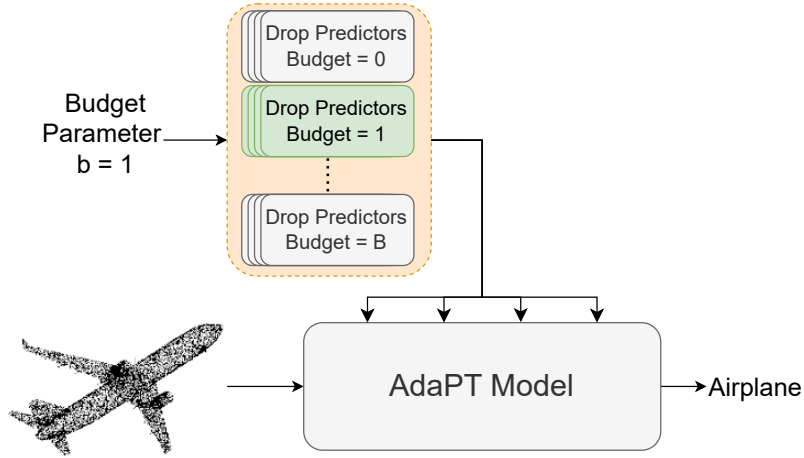


Figure 5: The budget parameter selects the set of drop predictors to be used in the classification of a point cloud. This parameter also selects a specific regularization term that is used to train the corresponding drop predictor set.

Let $b \in \{0, \dots, B\}$ be an index variable denoting increasingly higher budget values set by the user. We use t_i^b to denote the corresponding b -th desired budget at the i -th layer. In addition, denote by d_i^b the ratio of dropped tokens at layer i if we use the b -th drop predictor module. The regularization term in (3) becomes:

$$\mathcal{L}_{drop} = \sum_{b=1}^B \sum_{i=0}^p \frac{(d_i^b - t_i^b)^2}{p} \quad (5)$$

where we want all budgets to be simultaneously satisfied depending on the index b . Computing this regularization term is unfeasible because it would require B forward passes for each input point cloud (one for each budget). To this end, during training a random budget is extracted for each batch of data, and the corresponding regularization term and set of drop predictor modules are used for that batch.

During inference, the budget is an additional input required by the model, which selects the appropriate set of drop predictor modules. By selecting a set of modules trained with a certain regularization term, this parameter selects the ratio of tokens that will be eliminated during inference, hence selecting the computational budget for that prediction.

4. Experimental section

In this section, we compare our model to two other transformer-based architectures for point cloud classification, presented in Guo et al. (2021) and Zhao et al. (2021). The dataset used for these comparisons is ModelNet40 (Wu et al., 2015). To allow for a fair comparison of the results, we implemented the models used in these works into our pipeline, training and

testing the models on the same split of the dataset and with the same data preprocessing.

4.1. Regularization target and Budget parameter

We set the target used for the regularization presented in (3) using two hyperparameters: the number of layers with a drop predictor associated, ℓ , and the desired ratio of dropped tokens to initial tokens after the last layer, ρ . Once those parameters are fixed, the target ratio for each layer is computed as:

$$t_i = \frac{i}{\ell} \cdot \rho \quad i = 1, \dots, \ell \quad (6)$$

Additionally, we need to set the target for different values of the budget parameter. We choose to have the target depend linearly on the value of the budget parameter, so that the only hyperparameter to be set is the number of different budgets available, B . The targets associated to the different budgets are then computed as follows:

$$t_i^b = \frac{B-b}{B-1} \cdot t_i = \frac{(B-b) \cdot i}{(B-1) \cdot \ell} \cdot \rho \quad b = 1, \dots, B \quad i = 1, \dots, \ell \quad (7)$$

We set $\ell = 4$, $\rho = 0.8$, and $B = 4$ in our experiments. With our parameters choice, we obtain the targets in Tab. 4.1.

Each row of Tab. 4.1 corresponds to a target that will be used to train a set of drop predictor modules.

4.2. Point Cloud Classification on ModelNet40

ModelNet40 consists of 12,311 CAD models distributed across 40 object categories, making it a popular choice for benchmarking point cloud shape

$i \backslash b$	1	2	3	4
4	0	0	0	0
3	0.07	0.13	0.20	0.27
2	0.13	0.27	0.40	0.53
1	0.20	0.40	0.60	0.80

Table 1: Values of t_i^b for the hyperparameters chosen in our experiments. Every row corresponds to a set of drop predictors associated with the value b of the budget parameter.

classification. To ensure a fair comparison, we adopted the official split, allocating 9,843 objects for training and 2,468 for evaluation. We adopted the same sampling strategy described by Charles et al. (2017) to uniformly sample each object to 2048 points.

During training, a random translation in the range $[-0.2, 0.2]$, a scaling in the range $[0.67, 1.5]$, and a random input dropout were applied to augment the input data. During inference, no augmentation is applied to the data.

A batch size of 64 was used during training. The initial learning rate was set to 0.001, with a cosine annealing scheduler adjusting it at every epoch.

The experimental results for this classification task are presented in Table 4.2. We can see that our model performs similarly to analogous transformer-based models. More importantly, we can see that our model does not suffer a significant loss of performance when the token drop is introduced. We can also see that the performance is approximately stable across all the different tested budgets, as shown visually in Fig. 6. We underline again that the results in Fig. 6 with the *same* model while varying the budget as

an input parameter.

Model	Accuracy
PCT	91.0
Point Transformer	90.8
AdaPT _{b=4}	90.1
AdaPT _{b=3}	89.8
AdaPT _{b=2}	89.5
AdaPT _{b=1}	89.4

Table 2: Shape classification results on the ModelNet40 dataset.

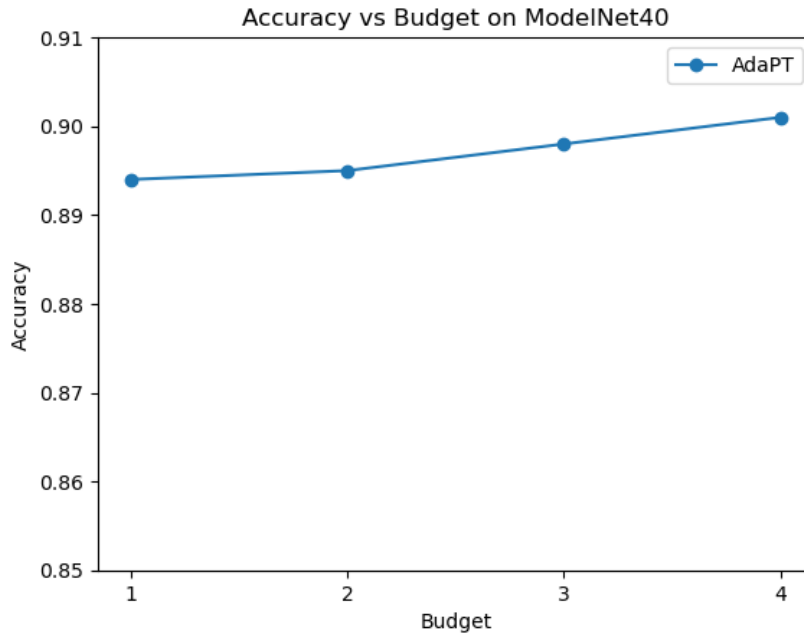


Figure 6: Model performance when selecting different budgets. A stronger budget means more eliminated tokens at each layer. We can see that the model manages to keep a stable performance when the intensity of the budget varies.

4.3. Flops count evaluation

We evaluated the inference FLOPS required by our model while varying the number of initial tokens.² Even though the regularization term in (3) pushes the model towards the desired number of dropped tokens, this number is not fixed during training. During inference, the number of tokens to be kept at each layer is deterministic, and the dropped tokens are completely eliminated, making it possible to count the model’s flop reliably.

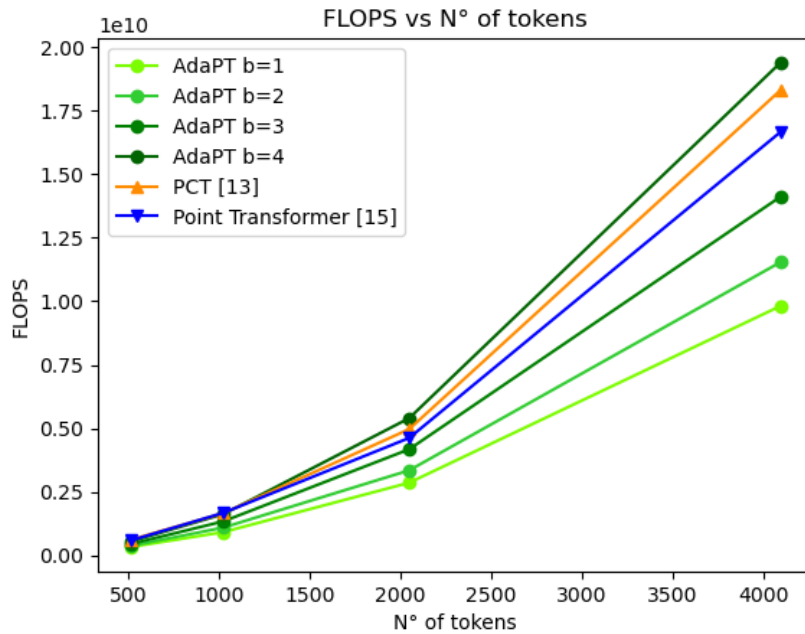


Figure 7: Flops in function of the number of tokens in the transformer part of the model.

The results are shown in Figure 7. As expected, our model is significantly more efficient when eliminating tokens.

²To evaluate the computational efficiency of our model, we calculate the inference flops using the FlopCountAnalysis method from the fvcore library.

We further investigated the effect of token selection on the model’s performance. We trained the model with different values of the hyperparameter ρ and observed the accuracy on the ModelNet40 classification task. We only consider the highest possible value for the budget parameter in these experiments. The result of these experiments are shown in Figure 8. As expected, we observe a trade-off between model accuracy and number of dropped tokens. We also observe a significant drop in performance when the drop target is set too high, requiring the model to eliminate 95% of the tokens in the last layer.

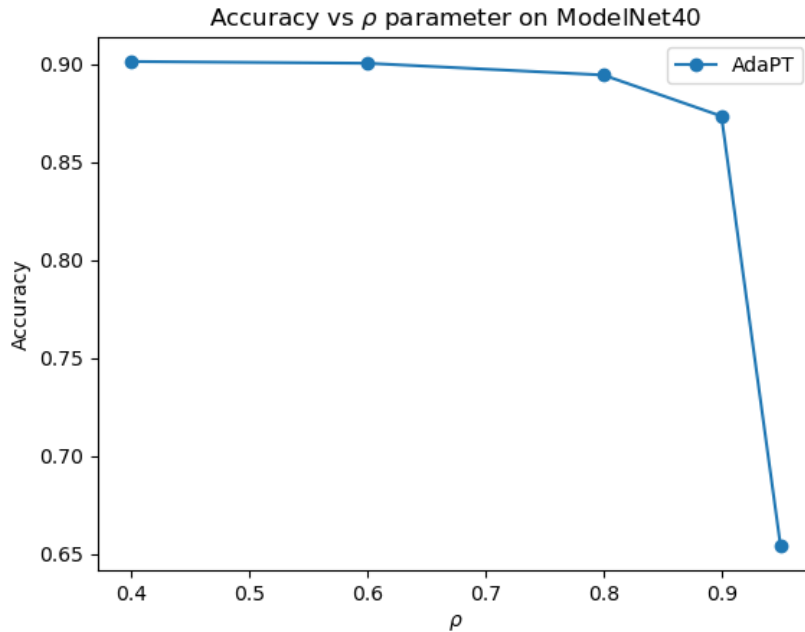


Figure 8: Accuracy of the model in the shape classification task on the ModelNet40 dataset as a function of the ρ hyper-parameter.

4.4. Ablation studies

In this section, we present additional experiments aimed at investigating the effectiveness and robustness of our model. To conduct these experiments, we fix the budget parameter to $b = 1$, corresponding to the most severe drop targets.

To test the effectiveness of our sampling strategy, we replace it with alternative, simpler sampling methods. In particular, we tested two different setups as alternatives to our method of token selection:

- **Random Selection:** the drop predictor selections are replaced by random samplings of the tokens. This can be seen as a form of token dropout.
- **Farthest Point Sampling:** We perform farthest point sampling on the tokens, in place of the selection made by the drop predictors. We perform this sampling by computing distances with respect to the original points' tridimensional positions.

Both performed worse than our sampling strategy. This indicates that our sampling strategy succeeds in selecting more informative tokens than the other two non-learnable sampling methods. The results of this test are shown in Table 3.

Sampling strategy	Accuracy
Random	79.5
Farthest-Point	85.2
Adaptive	89.4

Table 3: Shape classification results on the ModelNet40 dataset using different sampling methods.

5. Conclusions

In this paper, we presented Adaptive Point cloud Transformer (AdaPT), a model for efficient point cloud classification. We employed an end-to-end learnable and task-agnostic sampling mechanism relying on the Gumbel-Softmax distribution to achieve differentiable sampling. Moreover, we designed a budget mechanism capable of regulating the model’s inference FLOPS without retraining. Results on the benchmark dataset ModelNet40 for a point cloud classification task demonstrate the effectiveness of the proposed model.

Future developments of this work include extending the model’s task capability to include point cloud segmentation and further investigating the impact of learnable point subsampling on the model’s interpretability.

Declaration of competing interest

No author associated with this paper has any potential or pertinent conflicts which may be perceived to have impending conflicts with this work.

References

- E. Camuffo, D. Mari, S. Milani, Recent advancements in learning algorithms for point clouds: An updated overview, *Sensors* 22 (2022).
- T. N. Kipf, M. Welling, Semi-supervised classification with graph convolutional networks, in: *International Conference on Learning Representations (ICLR)*, 2017.
- R. Q. Charles, H. Su, M. Kaichun, L. J. Guibas, Pointnet: Deep learning on point sets for 3d classification and segmentation, in: *2017 IEEE Conference on Computer Vision and Pattern Recognition (CVPR)*, 2017, pp. 77–85.
- C. R. Qi, L. Yi, H. Su, L. J. Guibas, Pointnet++: Deep hierarchical feature learning on point sets in a metric space, in: I. Guyon, U. V. Luxburg, S. Bengio, H. Wallach, R. Fergus, S. Vishwanathan, R. Garnett (Eds.), *Advances in Neural Information Processing Systems*, volume 30, Curran Associates, Inc., 2017.
- Y. Guo, H. Wang, Q. Hu, H. Liu, L. Liu, M. Bennamoun, Deep learning for 3d point clouds: A survey, *IEEE transactions on pattern analysis and machine intelligence* 43 (2020) 4338–4364.
- A. Vaswani, N. Shazeer, N. Parmar, J. Uszkoreit, L. Jones, A. N. Gomez, L. u. Kaiser, I. Polosukhin, Attention is all you need, in: I. Guyon, U. V. Luxburg, S. Bengio, H. Wallach, R. Fergus, S. Vishwanathan, R. Garnett (Eds.), *Advances in Neural Information Processing Systems*, volume 30, Curran Associates, Inc., 2017.

- M.-H. Guo, J.-X. Cai, Z.-N. Liu, T.-J. Mu, R. R. Martin, S.-M. Hu, PCT: Point cloud transformer, *Computational Visual Media* 7 (2021) 187–199.
- T. Hackel, N. Savinov, L. Ladicky, J. D. Wegner, K. Schindler, M. Pollefeys, SEMANTIC3D.NET: A new large-scale point cloud classification benchmark, in: *ISPRS Annals of the Photogrammetry, Remote Sensing and Spatial Information Sciences*, volume IV-1-W1, 2017, pp. 91–98.
- L. Zhang, R. Dong, H.-S. Tai, K. Ma, PointDistiller: Structured knowledge distillation towards efficient and compact 3d detection, in: *2023 IEEE/CVF Conference on Computer Vision and Pattern Recognition (CVPR)*, 2023, pp. 21791–21801.
- Y. Yao, Y. Zhang, Z. Yin, J. Luo, W. Ouyang, X. Huang, 3d point cloud pre-training with knowledge distillation from 2d images, 2022. [arXiv:2212.08974](https://arxiv.org/abs/2212.08974).
- L. Meng, H. Li, B.-C. Chen, S. Lan, Z. Wu, Y.-G. Jiang, S.-N. Lim, AdaViT: Adaptive vision transformers for efficient image recognition, in: *2022 IEEE/CVF Conference on Computer Vision and Pattern Recognition (CVPR)*, 2022, pp. 12299–12308.
- Y. Rao, W. Zhao, B. Liu, J. Lu, J. Zhou, C.-J. Hsieh, DynamicViT: Efficient vision transformers with dynamic token sparsification, in: *Advances in Neural Information Processing Systems (NeurIPS)*, 2021.
- J. Yang, Q. Zhang, B. Ni, L. Li, J. Liu, M. Zhou, Q. Tian, Modeling point clouds with self-attention and gumbel subset sampling, in:

- 2019 IEEE/CVF Conference on Computer Vision and Pattern Recognition (CVPR), 2019, pp. 3318–3327.
- B. Graham, M. Engelcke, L. v. d. Maaten, 3d semantic segmentation with submanifold sparse convolutional networks, in: 2018 IEEE/CVF Conference on Computer Vision and Pattern Recognition, 2018, pp. 9224–9232.
- G. Riegler, A. O. Ulusoy, A. Geiger, Octnet: Learning deep 3d representations at high resolutions, in: 2017 IEEE Conference on Computer Vision and Pattern Recognition (CVPR), 2017, pp. 6620–6629.
- Y. Wang, Y. Sun, Z. Liu, S. E. Sarma, M. M. Bronstein, J. M. Solomon, Dynamic graph CNN for learning on point clouds, *ACM Trans. Graph.* 38 (2019).
- D. Narayanan, M. Shoeybi, J. Casper, P. LeGresley, M. Patwary, V. Korthikanti, D. Vainbrand, P. Kashinkunti, J. Bernauer, B. Catanzaro, A. Phanishayee, M. Zaharia, Efficient large-scale language model training on GPU clusters using megatron-LM, in: *Proceedings of the International Conference for High Performance Computing, Networking, Storage and Analysis, SC '21*, Association for Computing Machinery, New York, NY, USA, 2021.
- S. Islam, H. Elmekki, A. Elsebai, J. Bentahar, N. Drawel, G. Rjoub, W. Pedrycz, A comprehensive survey on applications of transformers for deep learning tasks, *Expert Systems with Applications* 241 (2024) 122666.
- A. Dosovitskiy, L. Beyer, A. Kolesnikov, D. Weissenborn, X. Zhai, T. Unterthiner, M. Dehghani, M. Minderer, G. Heigold, S. Gelly, J. Uszkoreit,

- N. Houlsby, An image is worth 16x16 words: Transformers for image recognition at scale, in: International Conference on Learning Representations, 2021.
- H. Thisanke, C. Deshan, K. Chamith, S. Seneviratne, R. Vidanaarachchi, D. Herath, Semantic segmentation using vision transformers: A survey, *Engineering Applications of Artificial Intelligence* 126 (2023) 106669.
- L. Müller, C. Morris, M. Galkin, L. Rampásek, Attending to Graph Transformers, Arxiv preprint (2023).
- J. Zeng, D. Wang, P. Chen, A survey on transformers for point cloud processing: An updated overview, *IEEE Access* 10 (2022) 86510–86527.
- H. Zhao, L. Jiang, J. Jia, P. Torr, V. Koltun, Point transformer, in: ICCV, 2021.
- F. Duman Keles, P. M. Wijewardena, C. Hegde, On the computational complexity of self-attention, in: S. Agrawal, F. Orabona (Eds.), *Proceedings of The 34th International Conference on Algorithmic Learning Theory*, volume 201 of *Proceedings of Machine Learning Research*, PMLR, 2023, pp. 597–619.
- D.-A. Clevert, T. Unterthiner, S. Hochreiter, Fast and accurate deep network learning by exponential linear units (ELUs)., in: ICLR (Poster), 2016.
- E. Jang, S. Gu, B. Poole, Categorical reparameterization with gumbel-softmax, in: International Conference on Learning Representations, 2017.

Z. Wu, S. Song, A. Khosla, F. Yu, L. Zhang, X. Tang, J. Xiao, 3d shapenets:
A deep representation for volumetric shapes, in: 2015 IEEE Conference on
Computer Vision and Pattern Recognition (CVPR), 2015, pp. 1912–1920.